

S.I. Seneviratne · J.S. Pal · E.A.B. Eltahir · C. Schär

Summer dryness in a warmer climate: a process study with a regional climate model

Received: 3 April 2001 / Accepted: 2 April 2002 / Published online: 8 June 2002
© Springer-Verlag 2002

Abstract Earlier GCM studies have expressed the concern that an enhancement of greenhouse warming might increase the occurrence of summer droughts in mid-latitudes, especially in southern Europe and central North America. This could represent a severe threat for agriculture in the regions concerned, where summer is the main growing season. These predictions must however be considered as uncertain, since most studies featuring enhanced summer dryness in mid-latitudes use very simple representations of the land-surface processes (“bucket” models), despite their key importance for the issue considered. The current study uses a regional climate model including a land-surface scheme of intermediate complexity to investigate the sensitivity of the summer climate to enhanced greenhouse warming over the American Midwest. A surrogate climate change scenario is used for the simulation of a warmer climate. The control runs are driven at the lateral boundaries and the sea surface by reanalysis data and observations, respectively. The warmer climate experiments are forced by a modified set of initial and lateral boundary conditions. The modifications consist of a uniform 3 K temperature increase and an attendant increase of specific humidity (unchanged relative humidity). This strategy maintains a similar dynamical forcing in the warmer climate experiments, thus allowing to investigate thermodynamical impacts of climate change in comparative isolation. The atmospheric CO₂ concentration of the sensitivity experiments is set to four times its pre-

industrial value. The simulations are conducted from March 15 to October 1st, for 4 years corresponding to drought (1988), normal (1986, 1990) and flood (1993) conditions. The numerical experiments do not present any great enhancement of summer drying under warmer climatic conditions. First, the overall changes in the hydrological cycle (especially evapotranspiration) are of small magnitude despite the strong forcing applied. Second, precipitation increases in spring lead to higher soil water recharge during this season, compensating for the enhanced soil moisture depletion occurring later in the year. Additional simulations replacing the plant control on transpiration with a bucket-type formulation presented increased soil drying in 1988, the drought year. This suggests that vegetation control on transpiration might play an important part in counteracting an enhancement of summer drying when soil water gets limited. Though further aspects of this issue would need investigating, our results underline the importance of land-surface processes in climate integrations and suggest that the risk of enhanced summer dryness in the region studied might be less acute than previously assumed, provided the North American general circulation does not change markedly with global warming.

1 Introduction

Earlier numerical studies with general circulation models (GCMs) have expressed the concern that rising concentrations of carbon dioxide and other greenhouse gases might increase the occurrence of summer droughts in mid-latitudes (e.g. Manabe et al. 1981; Wetherald and Manabe 1995, 1999). This could represent a severe threat for the agriculture of the regions concerned, where summer is the main growing season. The regions which might particularly be affected are southern Europe and central North America (e.g. Kattenberg et al. 1996). In this study we focus on the American Midwest, one of the agriculturally most productive areas in the world.

S.I. Seneviratne (✉) · C. Schär
Institute for Atmospheric and Climate Science,
Swiss Federal Institute of Technology (ETH),
8057 Zurich, Switzerland
E-mail: sonia@geo.unw.ethz.ch

J.S. Pal · E.A.B. Eltahir
Ralph M. Parsons Laboratory for Hydrodynamics
and Water Resources,
Department of Civil and Environmental Engineering,
Massachusetts Institute of Technology,
Cambridge, MA 02139, USA

The responsible mechanism was inferred by Wetherald and Manabe (1995; hereafter referred to as WM95). According to their analysis, enhanced greenhouse gas forcing leads to an increase in net surface radiation, which is primarily balanced by latent rather than sensible heat flux in the equatorward side of the mid-latitude rain belt (45°N–60°N). The increase in evapotranspiration accumulates during late spring and summer so as to deplete soil moisture. Towards late summer soil moisture becomes so low that evapotranspiration cannot increase any further, leading to an increase in sensible heat flux and an additional enhancement of surface temperature. Extra precipitation that occurs in winter and spring is unable to correct for this development, as the soil in the control and enhanced-CO₂ experiments is generally close to saturation at this time; this ensures that much of the extra precipitation occurring in the enhanced-CO₂ integrations is not stored in the soil but lost to runoff. Later increases in evapotranspiration can therefore not be counterbalanced.

In agreement with these hypotheses, various GCM studies feature enhanced summer dryness in mid-latitudes under increased atmospheric CO₂ concentrations (e.g. Rind et al. 1990; Kattenberg et al. 1996; Gregory et al. 1997; Cubasch et al. 2001). Transient climate change experiments accounting for future changes in aerosol concentrations yield a somewhat delayed response but qualitatively similar results (Wetherald and Manabe 1999). Accordingly, the enhanced occurrence of summer drought in mid-latitudes, though not confirmed by observations up to now, is generally considered a likely (Cubasch et al. 2001) or very likely (Easterling et al. 2000) future consequence of climate change.

However, the simulation of the summer hydrological cycle over extratropical land-masses is a highly sensitive issue. Even with current atmospheric greenhouse gas concentrations, many models have a mild or even strong summer drying. This problem affects free GCM simulations with prescribed sea surface temperatures (e.g. Wild et al. 1996), regional climate models driven by observed lateral boundary conditions (e.g. Machenhauer et al. 1998), and even weather forecasting models (Betts et al. 1996). Substantial research was devoted to clarify the source of this problem, which proves a difficult task as many model aspects appear relevant (radiation, clouds, convective precipitation, land-surface processes). For the ECHAM3 atmospheric GCM, Wild et al. (1995, 1996) identified excessive solar radiation as one of the key problems, and demonstrated how improving the respective parametrization did largely reduce summer dryness. Another possible source of the summer dryness problem within simulations of the present climate is in the parametrization of convective clouds and their interaction with evapotranspiration. Dry soils can promote a reduction of convective precipitation, and this feedback may further amplify soil moisture loss. The underlying feedback is known to be sensitive to a wide range of processes, including cloud-radiation interaction (Findell and Eltahir 1997; Schär et al. 1999; Heck et al. 2001).

Finally, as pointed out by Kattenberg et al. (1996), most climate change studies featuring enhanced summer dryness use very simple representations of the land surface (“bucket” models; see Manabe 1969). The bucket model is known to overestimate evaporation over bare ground and for dry conditions over vegetated areas (Viterbo 1996). It does also overestimate daytime evaporation when energy and soil moisture are available (Dickinson and Henderson-Sellers 1988; Henderson-Sellers et al. 1996). These characteristics may exaggerate summer dryness in climate change experiments employing a bucket parametrization of the land-surface hydrology (Gates et al. 1996; Kattenberg et al. 1996). In contrast, Déqué et al. (1998), who use a more sophisticated land-surface parametrization in climate change simulations with a variable resolution GCM, find only little climate change impact upon soil moisture over Europe. It is thus desirable to investigate this issue with models that include realistic representations of the shortwave radiation, precipitation and land-surface processes.

Here we use a regional climate model (RCM) with a land-surface scheme of intermediate complexity (the Biosphere–Atmosphere Transfer Scheme BATS, see Dickinson et al. 1993), to investigate this issue over the Midwestern United States. We use the methodology of surrogate climate scenario proposed by Schär et al. (1996) for the simulation of warmer climatic conditions. The procedure is distinct from GCM-based climate change scenarios. The control (CTL) simulations are initialized and driven at their lateral and sea surface boundaries by observations and reanalysis data. The warm climate scenario investigates a hypothetical climate state with enhanced air and surface temperature, unchanged relative humidity and increased CO₂ concentrations. The methodology consists of driving the warm climate experiments (WARM) by a modified set of initial and lateral boundary conditions characterized by a uniform warming of 3 K and an attendant shift in absolute humidity (consistent with unchanged relative humidity). In essence, the driving fields of the WARM and CTL simulations are dynamically identical, but characterized by shifts in temperature and absolute humidity. The two scenarios may therefore be associated with different hydrological cycles within the model domain, while presenting similar synoptic patterns. This methodology is well suited to investigate a complex loop of physical feedback processes, since ambiguities due to different synoptic settings are minimized by design. The simulations are conducted over the contiguous United States for the springs and summers of four years, representing drought (1988), normal (1986, 1990), and flood (1993) conditions.

2 Model description

The present experiments are performed with a modified version of the National Center for Atmospheric Research’s Regional Climate

Model (RegCM); a detailed description of the NCAR RegCM can be found in Giorgi et al. (1993a, b) and Giorgi and Mearns (1999). Here we briefly summarize the main features of the model employed.

RegCM is built upon the NCAR-Pennsylvania State University (NCAR-PSU) Mesoscale Model version 4 (MM4; Anthes et al. 1987). It is a hydrostatic primitive equation model in σ_p vertical coordinates. Here $\sigma_p = (p - p_{top}) / (p_s - p_{top})$, where p is pressure, p_{top} is the pressure specified at the top of the model, and p_s is the prognostic surface pressure. For our experiments, p_{top} is 50 mbar and 14 levels in the vertical are specified.

Large-scale clouds and precipitation are represented using the sub-grid explicit moisture scheme (SUBEX) developed by Pal et al. (2000). Cumulus convection is represented using the Grell parametrization (Grell 1993; Grell et al. 1994) in which the Fritsch-Chappell closure assumption (Fritsch and Chappell 1980) is implemented. The atmospheric radiative transfer computations are performed using the formulation from NCAR's Community Climate Model version 3 (CCM3; Kiehl et al. 1998) with the inclusion of an additional routine accounting for changes in the concentrations of trace gases (E.E. Small, personal communication 1998). The planetary boundary layer computations are performed using the non-local formulation of Holtslag et al. (1990).

The Biosphere–Atmosphere Transfer Scheme version 1e (BATS1e; Dickinson et al. 1993) is used for the surface physics calculations. BATS describes the exchange of heat, moisture and momentum between the atmosphere and the land surface. It comprises one vegetation canopy layer, three soil layers and one snow layer. The soil layers comprise a 10 cm surface layer, a 1, 1.5 or 2 m root zone (depending on the vegetation type), and a 3 m deep soil layer; all layers start from the surface, i.e. the deep soil layer includes both the root layer and the surface layer, and the root layer includes the surface layer.

Evapotranspiration over land in BATS originates from three sources: bare soil evaporation from the top soil layer, transpiration from the root zone (dry leaves), and potential evaporation from the interception layer (wet leaves). Transpiration (E_{TR}) is by far the largest of the three terms in mid-latitude spring and summer. It is expressed as follows: $E_{TR} = \frac{r_{la}}{r_{la} + r_s} E_{pot}$, where r_{la} is the aerodynamic resistance to moisture and heat transfer through the boundary layer

at the foliage surface, r_s is the stomatal resistance, and E_{pot} is the potential evaporation.

The stomatal resistance r_s is the resistance of foliage to water vapour transfer. BATS follows the Jarvis-type approach (Jarvis 1976) for its computation: $r_s = r_{smin} R_f S_f M_f V_f$, where the factors R_f , S_f , M_f and V_f give the dependence of r_s on solar radiation, seasonal temperature evolution, moisture content and vapor pressure deficit, respectively. Under stress-free conditions, all four factors are equal to 1 and r_s is equal to the minimum stomatal resistance r_{smin} . An upper limit, r_{smax} , is also specified.

Transpiration is further limited in BATS by the root resistance to water uptake. A maximum transpiration rate E_{TRmax} is defined using a non-linear function of the soil water content.

A modification used in the present model version is a revised specification of minimum stomatal resistance based on the existing literature. BATS specifies r_{smin} values of 120 s/m for crops, 150 s/m for evergreen broadleaf trees, and 200 s/m for all other land cover/vegetation types (including forests and grasslands). These values appear to be too high in view of observations (e.g. Rowntree 1991), results from back-interpolation studies (Dorman and Sellers 1989) or typical modelling applications (e.g. Jacquemin and Noilhan 1990). Here, we use new specifications of r_{smin} of 40 s/m for crops and 80 s/m for all other vegetation types. These values appear to be closer to the aforementioned estimates and observations. The control and sensitivity experiments were conducted for both settings of r_{smin} . The modification shows little impact on the control integrations, except in 1993 where it leads to a better prediction of the Midwestern flood, and the impact on the sensitivity experiments is small as well.

3 Design of numerical experiments

A summary of the experiments performed can be found in Table 1. The control and sensitivity experiments are initialized on March 15 for each of the following years: 1986, 1988, 1990, and 1993. The runs are integrated until October 1st, i.e. for a period of 200 days (6 1/2 months).

Table 1 CTL, WARM, BUCKTRA_CTL, BUCKTRA_WARM, and NOCO₂ experiments

Experiments	Initial and boundary fields				Atmospheric CO ₂	Transpiration parametrization
	Air temperature	Sea surface temperature	Relative humidity	Other fields ^a		
CTL86	TA86	SST86	RH86	INBC86	348 ppmv	BATS
CTL88	TA88	SST88	RH88	INBC88	351 ppmv	
CTL90	TA90	SST90	RH90	INBC90	354 ppmv	
CTL93	TA93	SST93	RH93	INBC93	359 ppmv	
WARM86	TA86 + 3K	SST86 + 3K	RH86	INBC86	1120 ppmv	BATS
WARM88	TA88 + 3K	SST88 + 3K	RH88	INBC88	1120 ppmv	
WARM90	TA90 + 3K	SST90 + 3K	RH90	INBC90	1120 ppmv	
WARM93	TA93 + 3K	SST93 + 3K	RH93	INBC93	1120 ppmv	
BUCKTRA_CTL86	TA86	SST86	RH86	INBC86	348 ppmv	Bucket-type
BUCKTRA_CTL88	TA88	SST88	RH88	INBC88	351 ppmv	
BUCKTRA_CTL90	TA90	SST90	RH90	INBC90	354 ppmv	
BUCKTRA_CTL93	TA93	SST93	RH93	INBC93	359 ppmv	
BUCKTRA_WARM86	TA86 + 3K	SST86 + 3K	RH86	INBC86	1120 ppmv	Bucket-type
BUCKTRA_WARM88	TA88 + 3K	SST88 + 3K	RH88	INBC88	1120 ppmv	
BUCKTRA_WARM90	TA90 + 3K	SST90 + 3K	RH90	INBC90	1120 ppmv	
BUCKTRA_WARM93	TA93 + 3K	SST93 + 3K	RH93	INBC93	1120 ppmv	
NOCO ₂ 86	TA86 + 3K	SST86 + 3K	RH86	INBC86	348 ppmv	BATS
NOCO ₂ 88	TA88 + 3K	SST88 + 3K	RH88	INBC88	351 ppmv	
NOCO ₂ 90	TA90 + 3K	SST90 + 3K	RH90	INBC90	354 ppmv	
NOCO ₂ 93	TA93 + 3K	SST93 + 3K	RH93	INBC93	359 ppmv	

^aThe other initial and boundary fields (INBC) are the wind components, surface pressure, and soil moisture

The chosen years cover a wide range of historical hydrological situations over the American Midwest. While 1986 and 1990 can be considered “normal” years, 1988 was characterized by the warmest and driest summer experienced in the United States since 1936 (e.g. Ropelewski 1988), and the 1993 summer flooding over the American Midwest was one of the most devastating floods in modern history (e.g. Kunkel et al. 1994). The very different conditions which prevailed during these four years are for instance apparent from the top soil moisture (Fig. 1) and precipitation observations (Fig. 2).

The model domain covers all of the contiguous United States and parts of Canada and Mexico (see Fig. 3). The grid is defined on a rotated Mercator map projection. The domain is centred at 37.581°N and 95°W, and the origin of the map projection is rotated to 40°N and 95°W. It comprises 129E × 80NS grid points, with a horizontal grid spacing of 55.6 km (approximately half a degree). The region of focus for the analysis is the American Midwest (outlined in Fig. 3).

3.1 Control experiments

The control simulations for 1986, 1988, 1990, and 1993 (hereafter CTL86, CTL88, CTL90, and CTL93) are initialized and driven at their sea surface and lateral boundaries by observations and reanalysis data, respectively.

The initial and boundary conditions for wind, temperature, surface pressure, and water vapour are taken from the National Center for Environmental Prediction’s (NCEP) reanalysis data. The sea surface temperatures (SST) are taken from the United Kingdom

Meteorological Office (UKMO) SST dataset. The soil moisture dataset used to initialize the experiments (hereafter PE01) is described in Pal and Eltahir (2001). It is a merged dataset combining data from the Illinois State Water Survey (Hollinger and Isard 1994), a US derived soil moisture dataset (Huang et al. 1996), and a climatology based on vegetation types. The lateral boundaries are employed using a relaxation technique described in Davies and Turner (1977).

The atmospheric CO₂ concentrations of the control runs are set to the historical value of the respective simulation year; the values for 1986, 1988, 1990, and 1993 range between 350 and 360 ppmv (see Table 1).

3.2 WARM experiments

A surrogate climate change scenario following the methodology proposed by Schär et al. (1996) is used for the simulation of a warmer climate. The warm climate simulations for 1986, 1988, 1990, and 1993 (hereafter WARM86, WARM88, WARM90, and WARM93) are driven with the initial and boundary fields of the control runs, modified so that the atmospheric and sea surface temperatures are increased uniformly by 3 K, while the relative humidity remains unchanged (all other initial and boundary fields are identical for both sets of simulations). This modification results in a substantial increase of the specific humidity (approximately +21% for a temperature increase of +3 K), and retains the system’s characteristic dynamic and thermodynamic balances (Schär et al. 1996; Frei et al. 1998).

The atmospheric CO₂ concentration of the WARM simulations is set to four times its pre-industrial value (280 ppmv), i.e. 1120 ppmv. Thus the atmospheric CO₂ concentration of the WARM experiments is equal to about three times the concentration of the control runs (see Table 1).

We chose a particularly strong forcing in order to increase the “signal-to-noise ratio” in our experiments. This also allows a better comparison with the experiments of WM95, who use an even larger CO₂ forcing (300 ppmv in the control integrations and 1200 ppmv in the enhanced-CO₂ experiments). Their simulations also display a much larger warming than the temperature forcing applied in the present simulations (about +8 K increase in surface air temperature in global average). This should be kept in mind when comparing the results of these two studies.

The chosen procedure is useful for identifying key mechanisms induced by warmer climatic conditions, but also entails some limitations. In particular, the design of the experiments implies that the control and warmer climate integrations are characterized by similar synoptic climatologies. In reality, one expects that global warming will be associated with possibly significant changes in the location and amplitude of the storm tracks (e.g. Cubasch et al. 2001); that may in turn affect the frequency of droughts and floods (e.g. Mo et al.

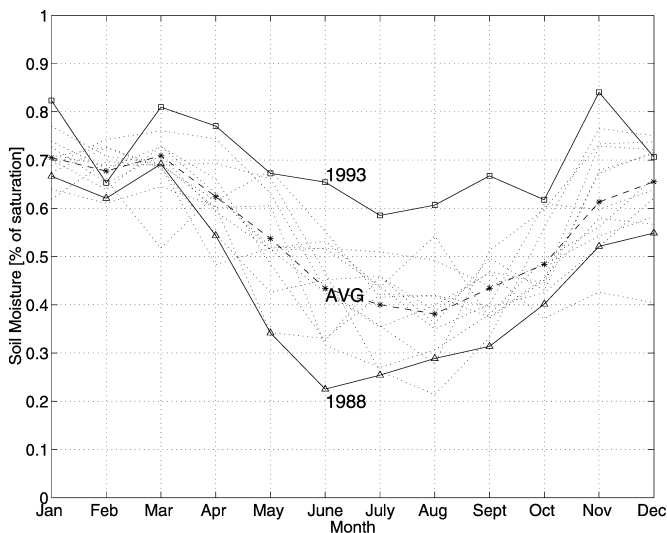


Fig. 1 Illinois State Water Survey monthly averaged relative soil moisture content from 0 to 10 cm for 1981 to 1993: 1988 (solid line with triangles); 1993 (solid line with squares); remaining years (dotted lines); average over all years (dashed line with asterisks). Data from Hollinger and Isard (1994)

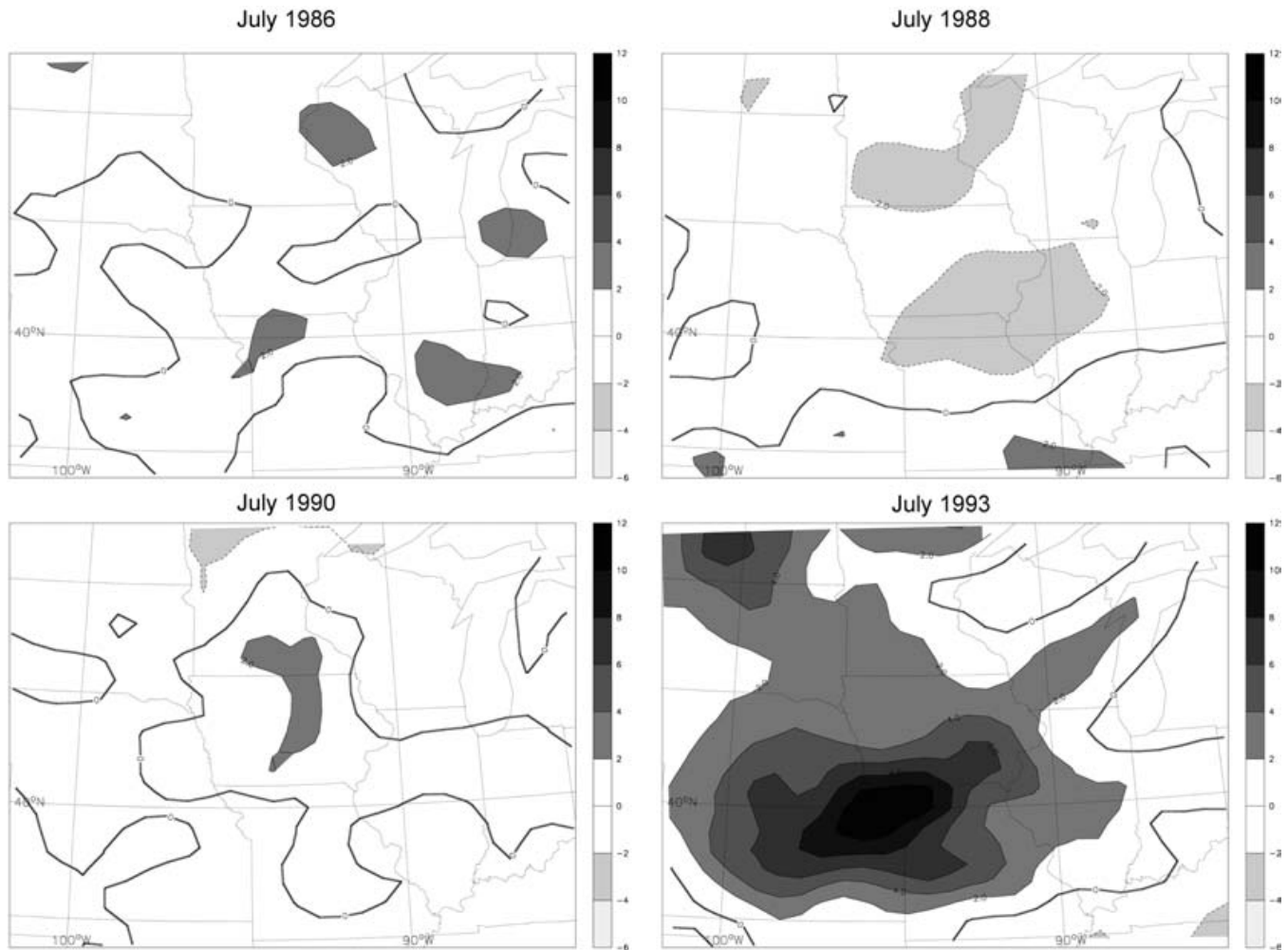


Fig. 2 Rainfall anomalies (mm/day) for July 1986, 1988, 1990, and 1993 over the American Midwest as derived from the USHCN data set (Karl et al. 1990) relative to a climatological value based on 16 years of observations (1980–1996). A weak spatial smoothing has been applied for display purposes. Shading occurs above and below anomalies of 2 mm/day

1997). We should however emphasize that the experiments are only constrained by the initial conditions and at the boundaries; since the model domain is fairly large, the simulations can still develop diverging circulation patterns in the interior. The idealized set-up of the WARM experiments nevertheless implies that they should not be viewed as predictions, but as an investigation of the thermodynamic climate change effects upon the mid-latitude summer climate.

3.3 BUCKTRA experiments

In order to assess the extent to which the land-surface parametrization is responsible for the sensitivity of the WARM experiments, additional integrations are conducted with a bucket-type formulation of transpiration. These sets of experiments will be referred to as BUCKTRA_CTL and BUCKTRA_WARM (see Table 1).

The bucket model (Manabe 1969) computes evaporation as $E = \beta E_{pot}$, where β , the “evaporative factor”

(Budyko 1974), is a function of the soil moisture content only and where E_{pot} denotes the potential evaporation. The β factor varies linearly between 0 and 1 and is defined as $\beta = \frac{W}{W_k}$, where W is the actual soil moisture content and W_k is the soil moisture content at which total evaporation is no longer considered to be limited by soil moisture availability. Manabe (1969) uses $W_k = 0.75 W_{FC}$, where W_{FC} is the field capacity.

In order to simulate a bucket-type behaviour of transpiration in BATS, the following two modifications are performed in the BUCKTRA experiments:

1. In BATS, transpiration (E_{TR}) is defined as: $E_{TR} = \frac{r_{la}}{r_{la}+r_s} E_{pot}$, (see Sect. 2). In the BUCKTRA simulations, the term $\frac{r_{la}}{r_{la}+r_s}$ is replaced by a β evaporative factor defined in the following manner: $\beta = \frac{W-W_{PWP}}{W_k-W_{PWP}}$, with $0 \leq \beta \leq 1$, where W is the soil moisture content, W_k is 0.75 times the field capacity, and W_{PWP} is the soil moisture content at the plant wilting point.
2. The upper limit for transpiration E_{TRmax} , which represents the impact of root resistance on the plant water uptake (see Sect. 2), is suppressed.

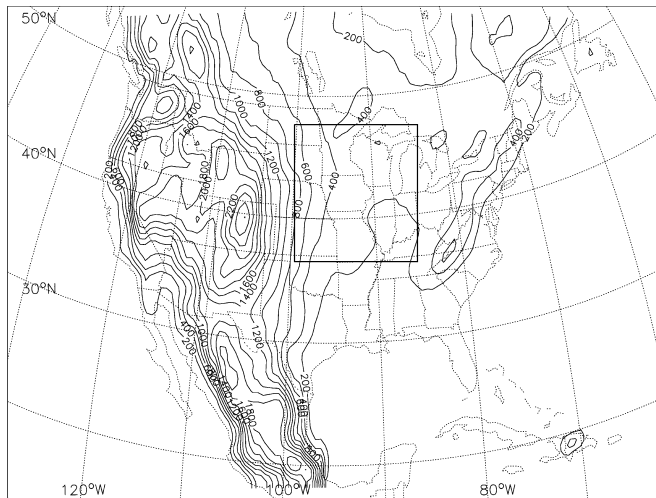


Fig. 3 Computational domain and topography (m) used for the numerical simulations. The Midwest analysis region (outlined box) is also indicated (approximately 36°N to 48°N, 99°W to 87°W)

These modifications replace the control imposed by stomatal and root resistances on transpiration by a single factor, depending on the soil moisture content only. Note that the BUCKTRA simulations still include bare soil evaporation and potential evaporation from the interception storage, which are considered of minor importance for the present comparisons. The role of further significant differences between the bucket model and the BATS land-surface scheme, such as the available water capacity or the treatment of runoff and groundwater drainage, are not investigated here, but might also be relevant to the issue.

3.4 NOCO₂ experiments

In order to quantify the relative impact of the local increase in atmospheric CO₂ concentration versus the thermodynamic modifications in the WARM experiments, additional simulations are conducted including the thermodynamic modifications only (warming of air temperature and SST by 3 K with unchanged relative humidity). This set of experiments uses the present-day values of the CO₂ concentrations and will be referred to as NOCO₂ (see Table 1 for a summary).

4 Control integrations

The validation of the control integrations is kept short, since the employed model version has been extensively validated in a similar setup by Pal (2001). In this section we focus therefore on the validation of precipitation against observations from the United States Historical Climate Network data set (USHCN; Karl et al. 1990) and on the comparison of the simulated evolution of evapotranspiration over the state of

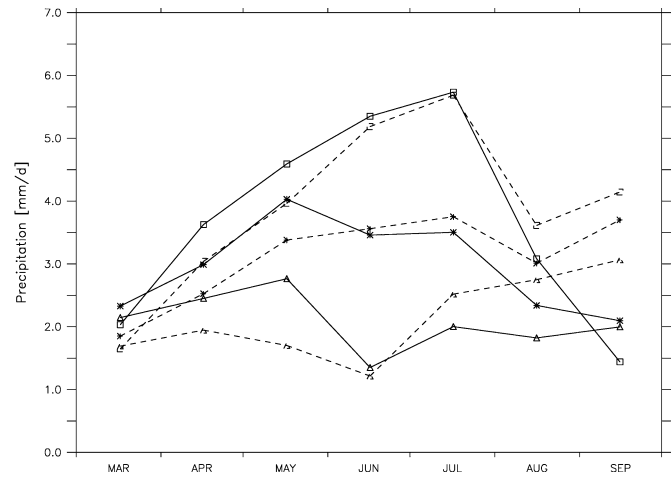


Fig. 4 Observed (dashed) and CTL (solid) monthly precipitation (mm/d) over the American Midwest for 1988 (triangles), 1993 (squares) and the average of the four years: 1986, 1988, 1990, and 1993 (asterisks). Observations are from the USHCN dataset (Karl et al. 1990). The values are spatial averages over the box outlined in Fig. 3

Illinois with estimates based on observational data (Yeh et al. 1998).

Figure 4 shows the temporal evolution of simulated precipitation over the Midwest for the extreme years (1988 and 1993) and the average of the four years. The model is able to capture the interannual variability of precipitation and simulates well the different evolutions observed in the normal and extreme years.

The spatial representation of precipitation over the whole domain is satisfactory as well; for illustration the predicted precipitation for two extreme dry and wet months, June 1988 and July 1993 respectively, are displayed in Fig. 5. The very low precipitation observed in June 1988 in the Midwestern United States is well captured by the model; there is however an underestimation of precipitation over Texas, Nebraska, and South Dakota during this month. Similarly, the rainfall peak of July 1993 over the Midwest is well captured, although somewhat shifted to the northeast; in the rest of the United States, precipitation is slightly underestimated. From these comparisons, we can conclude that the model captures precipitation variations satisfactorily, particularly over the Midwest focus region.

Since the simulation of evapotranspiration is of critical importance for the considered issue, we also compare the simulated evolution of evapotranspiration over the state of Illinois against the soil and atmospheric water balance estimates of Yeh et al. (1998). Figure 6 displays the temporal evolutions of the mean evapotranspiration in the CTL integrations over Illinois as well as the monthly evapotranspiration estimates. Though there seems to be an overestimation of evapotranspiration in spring (mostly in 1993, not shown), the simulated evolution of evapotranspiration is on the whole very satisfactory and in qualitative and quantitative agreement with the estimates.

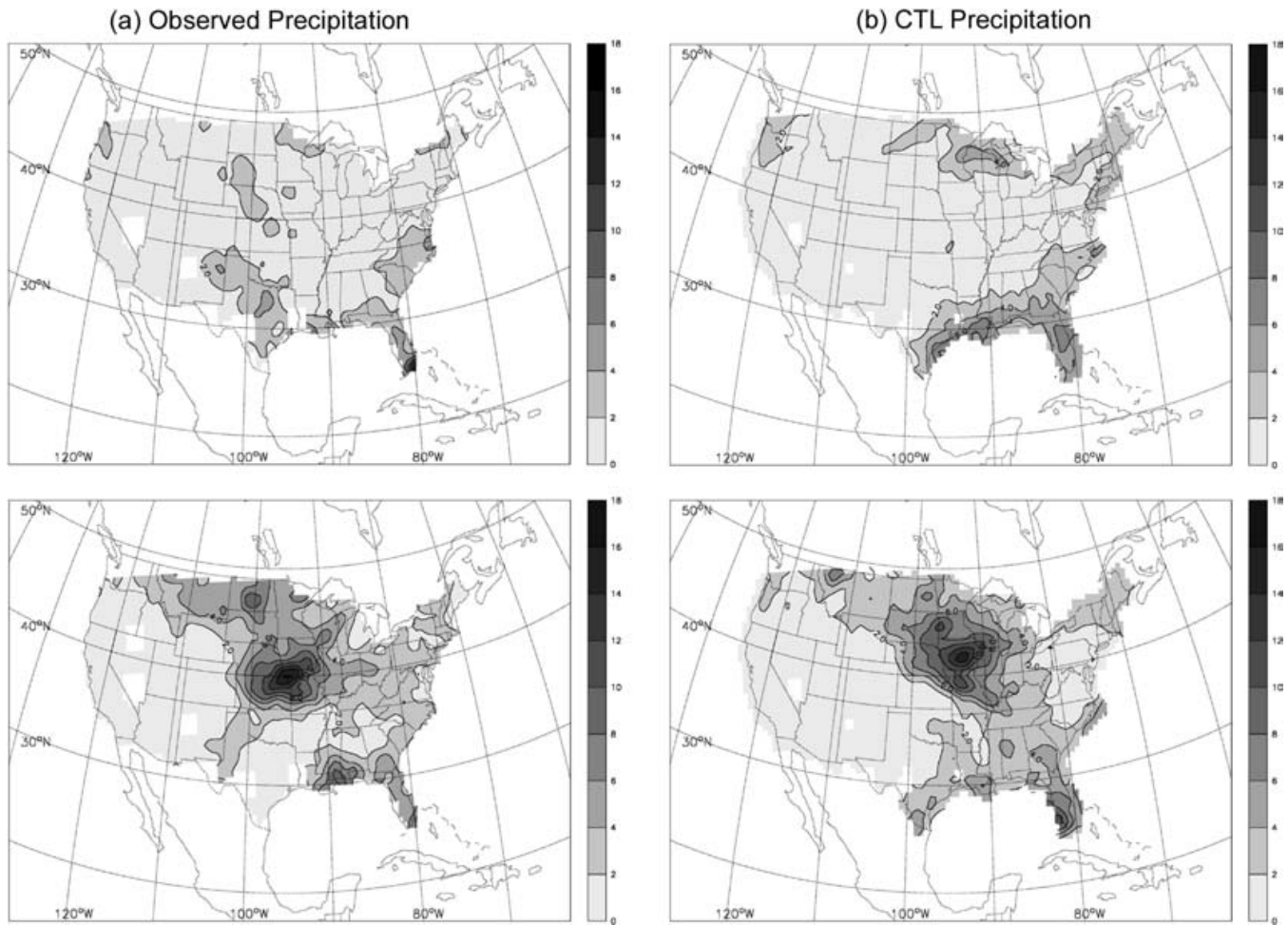


Fig. 5 a Observed and b CTL precipitation (mm/d) over the United States in June 1988 (top) and July 1993 (bottom). Observations are from the USHCN data set (Karl et al. 1990).

Note that the USHCN observations only exist over the United States. A weak spatial smoothing has been applied for display purposes

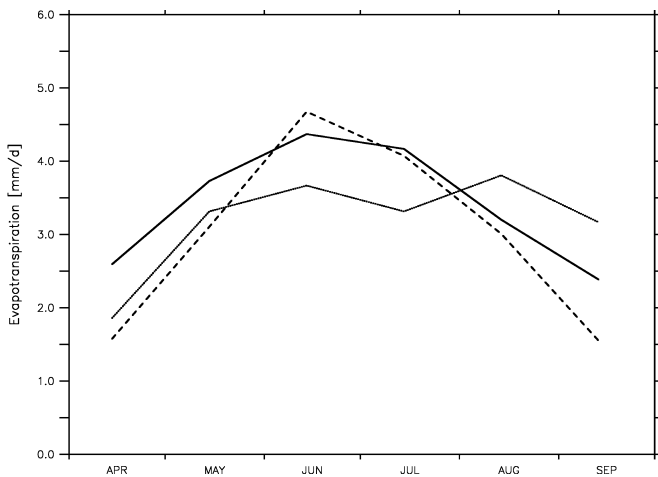


Fig. 6 Mean monthly land evapotranspiration in the CTL simulations (solid) averaged over Illinois (coordinates of subdomain: 36°N to 43°N and 93°W to 89°W) compared against atmospheric (dashed) and soil (dotted) water balance estimates based on observational data from 1983 to 1994 (Yeh et al. 1998). All values are in mm/d

5 Results of the sensitivity experiments

Unless otherwise specified, comparisons are made over a focus region centred on the American Midwest (see Fig. 3). This subdomain extends from about 36°N to 48°N, and 99°W to 87°W. Note that this region is located at lower latitudes than those investigated by WM95 (45°N to 60°N).

5.1 WARM experiments: hydrological cycle

The results of the integrations are summarized in Table 2 and compared against those of WM95 (Table 3). Figure 7 presents the mean temporal evolution of precipitation, evapotranspiration, and total runoff over the Midwest subdomain in the CTL and WARM integrations. The magnitude of the observed changes is small compared to the results of WM95. The highest differences in precipitation and evapotranspiration are of the

Table 2 Summary of the CTL and WARM experiments: mean of the four years simulated for the months of May, July and September. The values are spatial averages over the Midwest subdomain (outlined in Fig. 3). SWI denotes incident shortwave (SW) radiation, SWO outgoing SW, SWN net SW, LWI incident long-

wave (LW) radiation, LWO outgoing LW, LWN net LW, NR net radiation, LH latent heat flux, SH sensible heat flux, TS surface temperature, and RHA the anemometer relative humidity. Note that evaporation and runoff are negative and that energy fluxes directed downwards are counted positive

Fields	Units	May			July			September		
		CTL	WARM	Δ	CTL	WARM	Δ	CTL	WARM	Δ
Hydrological cycle										
Precipitation	mm/day	4.03	4.35	+0.32	3.50	3.44	-0.07	2.10	2.08	-0.02
Evaporation	mm/day	-3.47	-3.63	-0.16	-3.69	-3.95	-0.25	-2.16	-2.35	-0.19
Runoff	mm/day	-0.79	-0.85	-0.06	-0.52	-0.52	+0.00	-0.21	-0.19	+0.01
Snowmelt	mm/day	0.00	0.00	+0.00	0.00	0.00	+0.00	0.00	0.00	+0.00
Soil moisture	mm	438.5	440.1	+1.6	403.3	405.8	+2.5	383.6	378.2	-5.3
(root zone)	% sat	60.9	61.1	+0.3	55.8	56.2	+0.5	53.1	52.3	-0.8
Soil moisture (total)	mm	1079.8	1085.5	+5.8	1028.4	1035.5	+7.1	981.6	978.4	-3.3
	% sat	74.3	74.7	+0.4	70.8	71.2	+0.5	67.6	67.3	-0.2
Surface energy budget										
SWI	W/m ²	235.5	230.0	-5.5	262.1	267.5	+5.3	161.9	172.6	+10.6
SWO	W/m ²	-38.6	-37.8	+0.8	-44.0	-44.8	-0.8	-27.4	-29.4	-2.0
SWN	W/m ²	196.9	192.3	-4.6	218.1	222.6	+4.5	134.5	143.1	+8.6
LWI	W/m ²	323.0	342.1	+19.0	371.3	389.4	+18.1	337.5	354.8	+17.3
LWO	W/m ²	-387.5	-399.9	-12.4	-439.7	-454.8	-15.1	-397.3	-415.2	-17.9
LWN	W/m ²	-64.5	-57.8	+6.7	-68.4	-65.4	+3.0	-59.8	-60.4	-0.6
NR	W/m ²	132.4	134.4	+2.0	149.7	157.3	+7.5	74.7	82.7	+8.0
SH	W/m ²	-26.0	-23.7	+2.3	-43.0	-42.6	+0.4	-18.0	-20.5	-2.5
LH	W/m ²	-109.2	-107.5	-4.7	-109.5	-177.0	-7.5	-63.9	-69.6	-5.7
Surface climate										
TS	°C	14.3	16.6	+2.3	23.5	26.0	+2.5	16.1	19.3	+3.2
RHA	%	80.2	80.8	+0.6	70.1	67.4	-2.7	78.4	74.1	-4.3

order of 0.3 mm/day, while they are up to two or three times larger in the simulations of WM95 (Table 3). Particularly striking are the differences in spring evapotranspiration: while our simulations present an evapotranspiration increase of only 0.16 mm/d in May (Table 2), WM95 report an almost five time larger increase for this month (0.74 mm/d, Table 3). Moreover, runoff is almost unaffected in our simulations while very sensitiv in WM95.

Evapotranspiration is higher in the WARM experiments than in the CTL integrations in all the months simulated. Precipitation is higher in the WARM experiments from March to June due to an enhancement of convective activity during these months (see later). Later in the year (from July to September), precipitation differences between the CTL and WARM simulations are negligible.

The temporal evolution of the net input of water in the soil (precipitation–evaporation–runoff) over the Midwest subdomain is shown in Fig. 8a. From March to June, the precipitation increase is higher than the evapotranspiration increase; in May for instance, it is twice as high (Table 2). As the soil is not at saturation (Fig. 8b), this extra input of water can thus be stored in the soil. In July, the increase in evapotranspiration remains substantial, while precipitation is the same as in the CTL integrations. For this reason, there is an enhanced depletion of soil moisture during this month, but due to the higher storage of water during spring, soil moisture in the WARM simulations reaches lower values than in the CTL simulations by the end of August

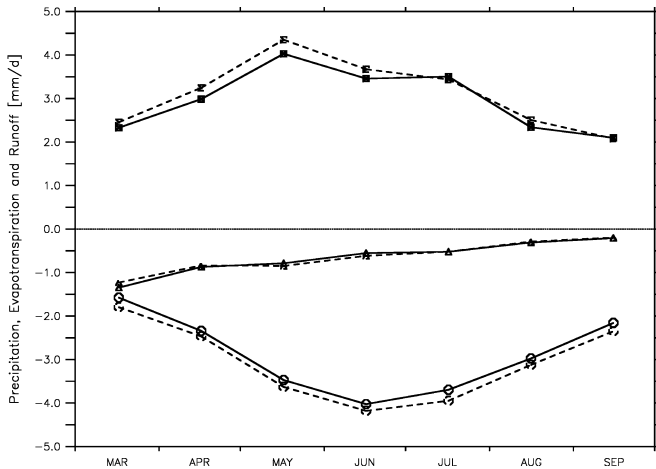
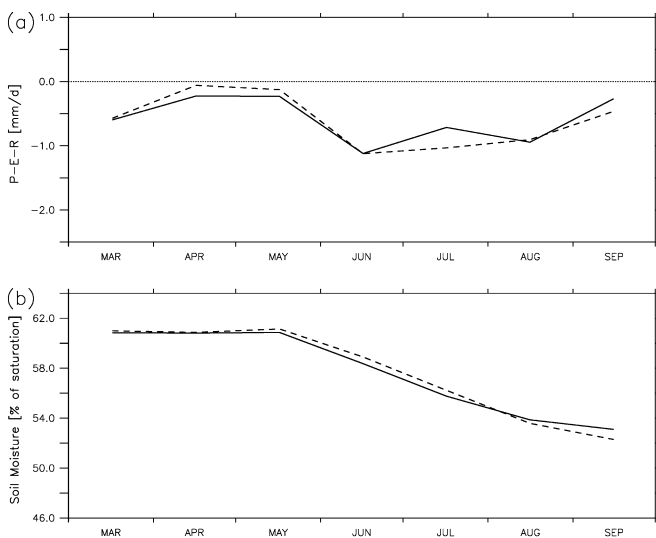
only. This sequence of events is clearly apparent in Fig. 8b which displays the temporal evolution of the soil moisture saturation in the root zone. Overall the differences between the CTL and WARM experiments are again very small. The highest (positive or negative) changes are of the order of 0.5–0.8% of soil saturation, corresponding to 2.5–5.5 mm in the root zone, the soil layer of relevance for plant growth (see Table 2 for exact values). In the total soil column, changes range from +7.1 mm (July) to -3.3 mm (September). In comparison, WM95 report mean soil moisture decreases of the order of 10 to 30 mm (see Table 3).

Figure 9 displays the geographical distribution of mean summer (June to August) soil moisture differences in the root zone (1 to 2 m depth) between WARM and CTL. There is no important drying in the focus region. Indeed, the highest drying peaks observed in the Midwest are of the order of 2% of the saturation water content, corresponding to 10–20 mm. Furthermore, many parts of this region display no changes in soil moisture at all, or even some signs of soil wetting (for instance in the states of Missouri, Kansas, and South and North Dakota). A possibly interesting feature is the large drying observed in the western Gulf Coast region around 30°N which is caused by a large decrease of summer precipitation (not shown).

Figure 10 displays the hydrological changes between the CTL and WARM experiments individually for each simulated year. The behaviour observed for the average of the simulations is again noticeable in 1986, 1988, and 1993: in all three years, there is an enhancement of

Table 3 Overview of the mean hydrological cycle (10 years) in Wetherald and Manabe (1995) based on simulations using a GCM with idealized geography for $1 \times \text{CO}_2$ (300 ppmv) and $4 \times \text{CO}_2$ (1200 ppmv, fully interactive experiment) equilibrium conditions. The figures represent averages for the continental region 45°N to 60°N . Sign conventions as in Table 2

Fields	Units	May			July			September		
		$1 \times \text{CO}_2$	$4 \times \text{CO}_2$	Δ	$1 \times \text{CO}_2$	$4 \times \text{CO}_2$	Δ	$1 \times \text{CO}_2$	$4 \times \text{CO}_2$	Δ
Precipitation	mm/day	3.33	3.89	+0.57	2.27	1.90	-0.37	2.40	2.73	+0.33
Evaporation	mm/day	-2.87	-3.61	-0.74	-3.19	-3.07	+0.13	-1.52	-1.63	-0.11
Runoff	mm/day	-2.65	-1.13	+1.52	-0.25	-0.11	+0.14	-0.18	-0.10	+0.08
Snowmelt	mm/day	1.76	0.00	-1.80	0.00	0.00	+0.0	0.04	0.00	+0.0
Soil moisture	mm	134.7	125.5	-9.2	61.9	35.3	-26.6	45.8	29.9	-15.9
(150 mm bucket)	% bucket	89.8	83.7	-6.1	41.3	23.5	-17.8	30.5	19.9	-10.6

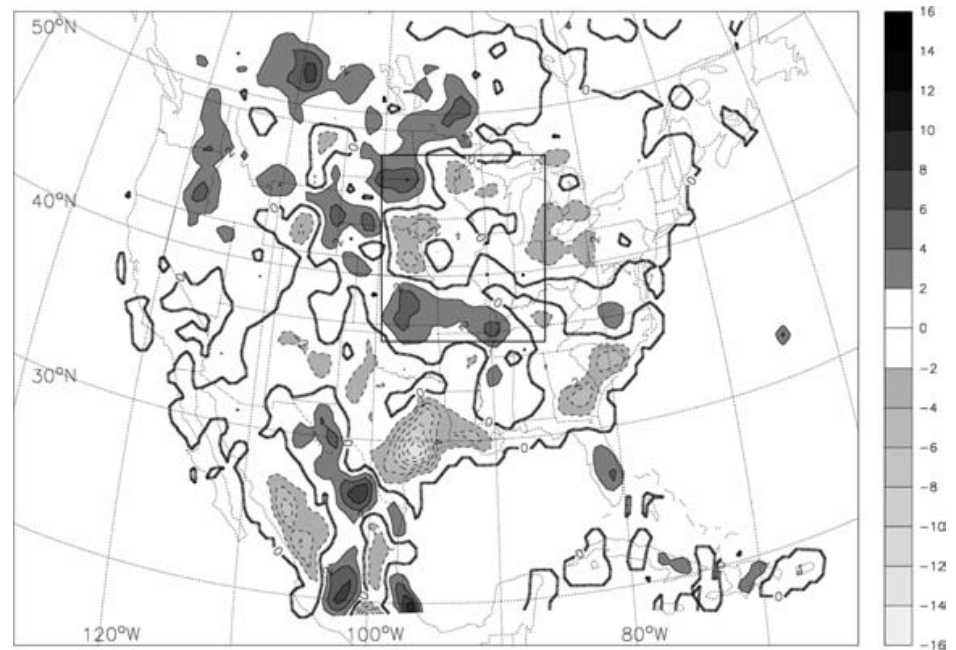
**Fig. 7** Temporal evolution of precipitation (*squares*), evapotranspiration (*circles*), and runoff (*triangles*) over the Midwest subdomain (outlined in Fig. 3) in the CTL (*solid*) and WARM (*dashed*) integrations (average over all years). The values are given in mm/day**Fig. 8** **a** Net input of water in the soil (precipitation-evapotranspiration-runoff) in mm/day. **b** Temporal evolution of the relative soil moisture content in the root zone in % of saturation. The values are averaged over the Midwest subdomain (outlined in Fig. 3) and represent means of the CTL (*solid lines*) and WARM (*dashed lines*) integrations

precipitation in spring leading to slightly wetter soil moisture conditions, which is followed by a gradual depletion of the additional soil water storage during the course of the summer. The applied scenario leads to an enhancement of the 1993 flood, while the 1988 drought conditions are not markedly different in the CTL and WARM integrations. In 1990, precipitation fails to increase sufficiently in spring to counterbalance the increase in evapotranspiration due to a decrease in large-scale precipitation in May; for this reason, somewhat enhanced summer drying occurs during this year. The opposite behaviour observed in the “normal” years (1986 and 1990) illustrate well the importance of the precipitation increase in spring. If the precipitation increase in spring is not high enough, then some minor summer drying might occur. Regardless of this effect, however, the absolute changes in soil moisture are of small magnitude in all four years considered.

A more detailed look at the temporal evolution of the convective and non-convective parts of precipitation (Fig. 11) shows that convective rainfall increases from March to June/July in all years. The precipitation increase observed in spring is therefore mainly due to increases in convection. Some changes in large-scale precipitation are observed in 1986 (increase) and 1990 (decrease). In May 1990, there is a significant decrease of large-scale precipitation, which is responsible for the absence of total precipitation increase in spring, and hence for the mild increase in summer drying observed in this year.

In summary, the hydrological changes in the WARM experiments are as follows: The simulations are generally characterized by a wetter spring with enhanced convective activity (from March to June/July), followed by a period with drier climatic conditions (July–September). Due to the higher infiltration associated with the enhanced spring precipitation and the relatively moderate increase in evapotranspiration, the simulated soil moisture changes are in general of very small magnitude. These results are independent of the choice of the closure assumption in the convection scheme, since additional experiments conducted with the Arakawa and Schubert (1974) closure assumption (not shown) were in qualitative agreement with the simulations presented.

Fig. 9 Average summer (June–August) changes in relative soil moisture content (% of saturation) in the root zone (1–2 m depth) for the 4 years simulated (WARM-CTL). *Shading* occurs above and below differences of +2% and –2% of saturation. A weak spatial smoothing has been applied for display purposes. The *box outlined* is the Midwest analysis region



5.2 WARM experiments: surface energy budget

Figure 12 presents the mean temporal evolution of the various components of the surface energy budget in the CTL and WARM integrations over the Midwest region. The differences for the net longwave radiation, the net shortwave radiation, the sensible heat flux, and the latent heat flux are shown in Fig. 13.

The average changes in the energy budget components are consistent with the changes observed in the hydrological cycle. There is a reduction of the incident shortwave radiation in spring. This is in agreement with the increase in convective activity observed in the WARM experiments and appears to be mainly induced by an increase of the low-level cloud amount and relative humidity, while the high cloud amount is decreased (not shown). As seen in the previous section, the latent heat flux (which is proportional to evapotranspiration) is increased for all the duration of the simulations due to the enhanced air temperature.

From March to June, the increase in latent heat flux occurs at the expense of sensible heat as the net radiation is almost equal in the two sets of integrations. The increase in incoming longwave radiation induced by the change in greenhouse gases (CO_2 and water vapour) is indeed almost entirely compensated by the combined effects of the enhanced outgoing longwave radiation (associated with the higher surface temperature) and the decrease in incoming shortwave radiation (due to increased low-level cloud cover and relative humidity).

From June onwards, there is an enhancement of the net radiation in the WARM experiments due to an increase in incident shortwave radiation; the latter is caused by a significant decrease in cloud amount, particularly in the lower part of the atmosphere (not

shown). The increase in net radiation is almost entirely converted into sensible heat, while latent heat does not markedly increase any further.

5.3 BUCKTRA experiments

Comparisons between the BUCKTRA and standard (CTL and WARM) experiments show that these two sets of experiments are similar in 1986, 1990, and 1993, but markedly distinct for the drought year 1988. Figure 14 displays the temporal evolution of transpiration and soil moisture in the root zone in 1988 for the simulations CTL, WARM, BUCKTRA_CTL, and BUCKTRA_WARM. For this year, transpiration is higher with the bucket-type formulation than with the standard BATS parametrization, both in the control (CTL, BUCKTRA_CTL) and warmer climate (WARM, BUCKTRA_WARM) runs. The BUCKTRA experiments display a large sensitivity to the applied climate change scenario, contrary to the experiments with the standard BATS parametrization: transpiration is markedly enhanced both in spring and summer, leading to a strong drying of the soil (see Fig. 14b, bottom). The drying starts in May, and attains about –5% of saturation (approximately –32 mm) until September. These figures are similar in magnitude to the changes reported by WM95. Note, however, that the differences for the average of the four years are much smaller, as the two sets of experiments differ significantly in 1988 only.

The fact that the performed changes only impact the results for 1988, the drought year, suggests that the vegetation control on transpiration in BATS (through root and stomatal resistances) mostly comes into play under water stress conditions. Conversely, this also

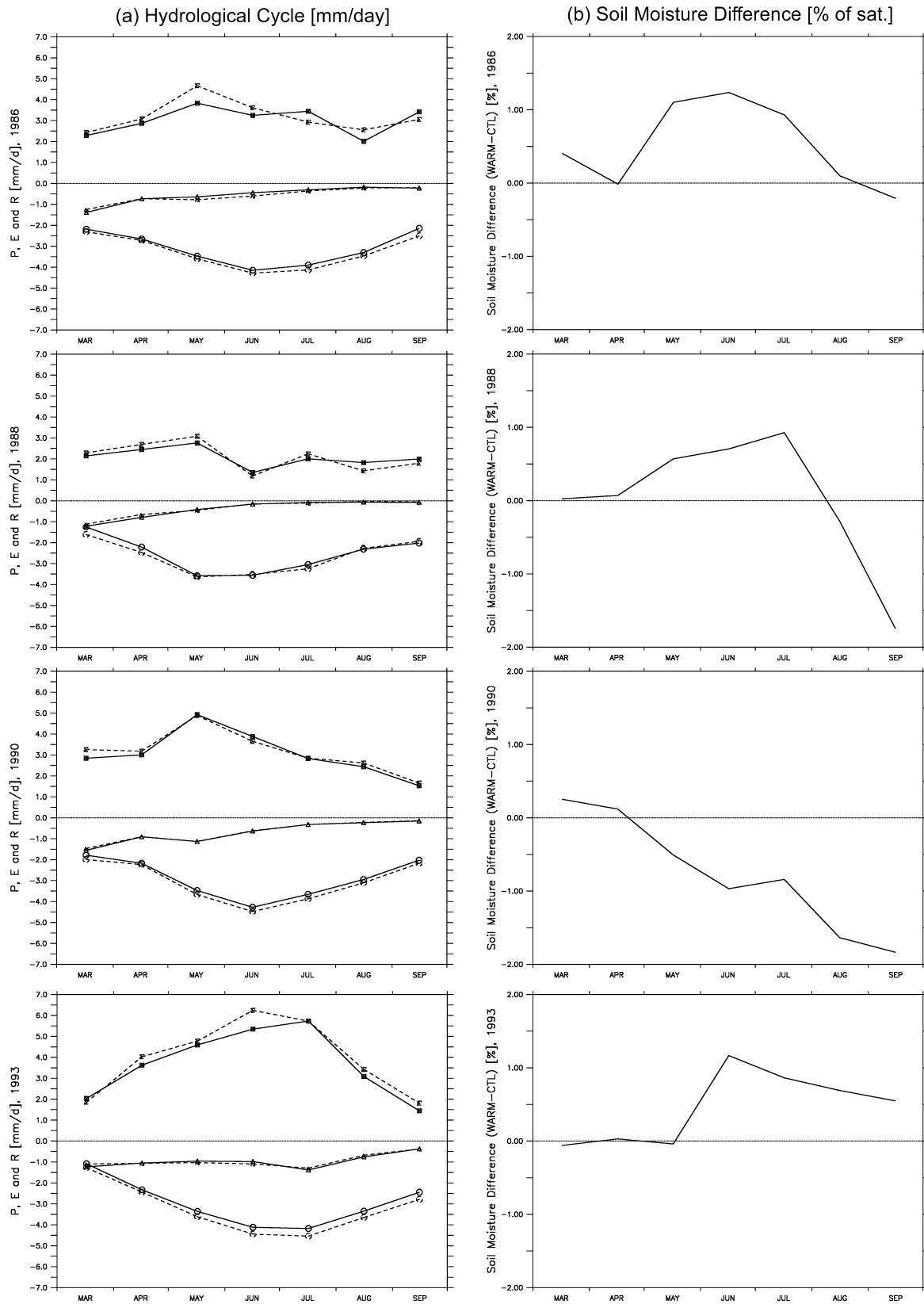


Fig. 10 a Temporal evolution of precipitation (*squares*), evapotranspiration (*circles*), and runoff (*triangles*) in the simulations CTL (*solid*) and WARM (*dashed*) in mm/day. b Temporal evolution of the soil moisture differences in the root zone (WARM-CTL) in %

of saturation. The values are spatial averages over the box outlined in Fig. 3. The *panels* represent 1986 (*top row*), 1988 (*second row*), 1990 (*third row*), and 1993 (*bottom row*)

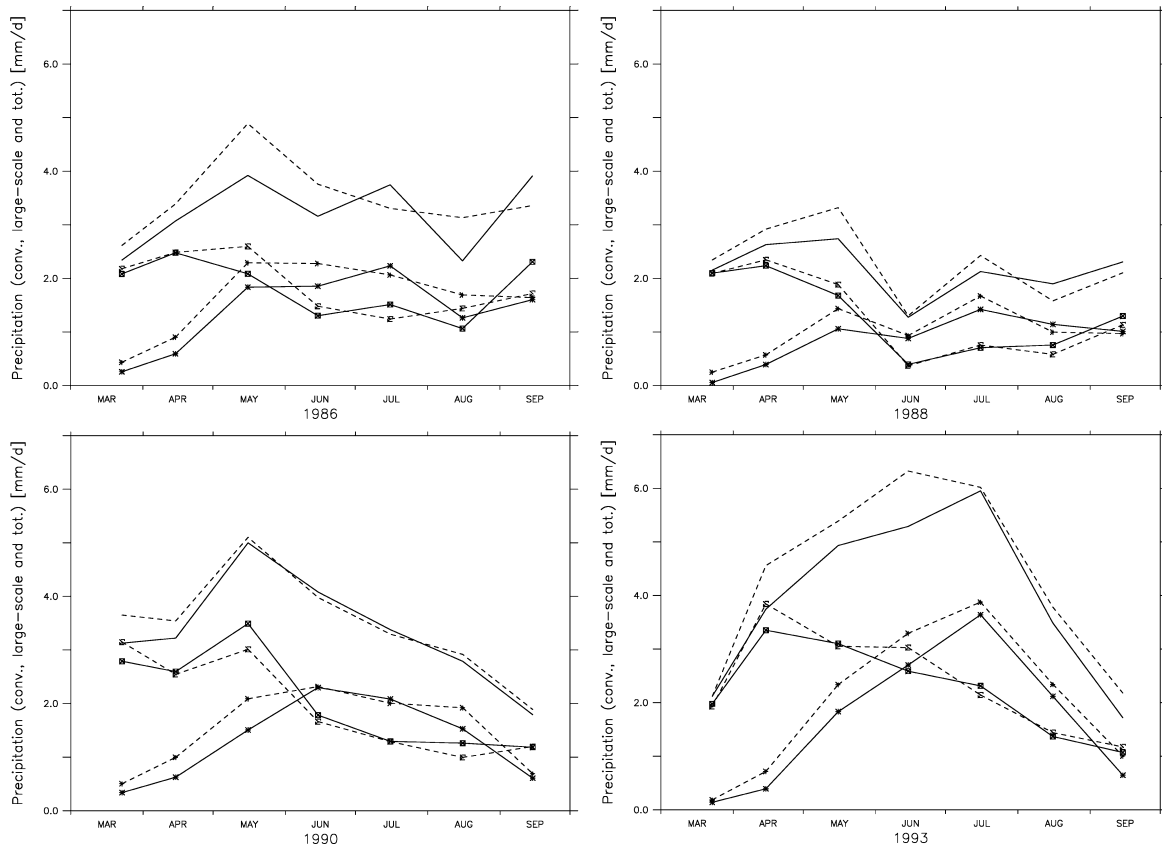


Fig. 11 Temporal evolution of total (no symbols), non-convective (squares), and convective rainfall (asterisks) in the simulations CTL (solid) and WARM (dashed) in 1986, 1988, 1990, and 1993 (mm/

day). The values are spatial averages over the Midwest subdomain (outlined in Fig. 3)

suggests that the bucket model might not be appropriate for investigating drought-like conditions.

As mentioned in Sect. 3, the changes performed in the BUCKTRA experiments do only mimic some of the characteristics of the bucket model; other aspects, such as the available water capacity and the treatment of runoff and groundwater drainage, would also need investigation. Despite these limitations, the results of the BUCKTRA experiments suggest that the more realistic land-surface scheme employed in our simulations might explain at least part of the differences observed between our study and earlier studies on this issue.

5.4 NOCO₂ experiments

Figure 15a displays the mean temporal evolution of the incident longwave radiation in the simulations CTL, WARM, and NOCO₂. The increase in incident longwave radiation exhibited by the WARM experiments (about +18 W/m²) is primarily induced by the enhanced moisture content of the atmosphere (80–90% of total change) rather than by the increase in atmospheric CO₂. This result is consistent with theory (e.g. Ramanathan 1981) and observations (e.g. Raval and Ramanathan 1989; Rind et al. 1991), since water vapour is known to

be a much more effective greenhouse gas than CO₂. The total increases in incident longwave radiation for both sets of simulations are also consistent with the results from GCM climate change simulations presented by Garatt et al. (1999). Their analysis of transient CO₂ experiments with three coupled climate models reveals indeed on a global average a mean increase of about 20 W/m² in incident longwave radiation for a 3 K increase in temperature.

Due to the limited impact of the differences in CO₂ concentrations, the results of the NOCO₂ experiments are therefore relatively similar to those of the WARM integrations, and are mostly characterized by their insensitivity to the performed changes. As an example, the temporal evolutions of the soil moisture differences in the root zone for WARM-CTL and NOCO₂-CTL are presented in Fig. 15b. As with the WARM simulations, the absolute change in soil moisture is very small (less than 2% of saturation). An analysis of the other fields shows that the amplitudes of the differences to the CTL runs are of similar magnitude (not shown).

We can conclude from this analysis that on the spatial and temporal scales considered, the differences between the WARM and CTL experiments can be mainly explained by the changes in temperature and specific humidity (through temperature advection and water vapour

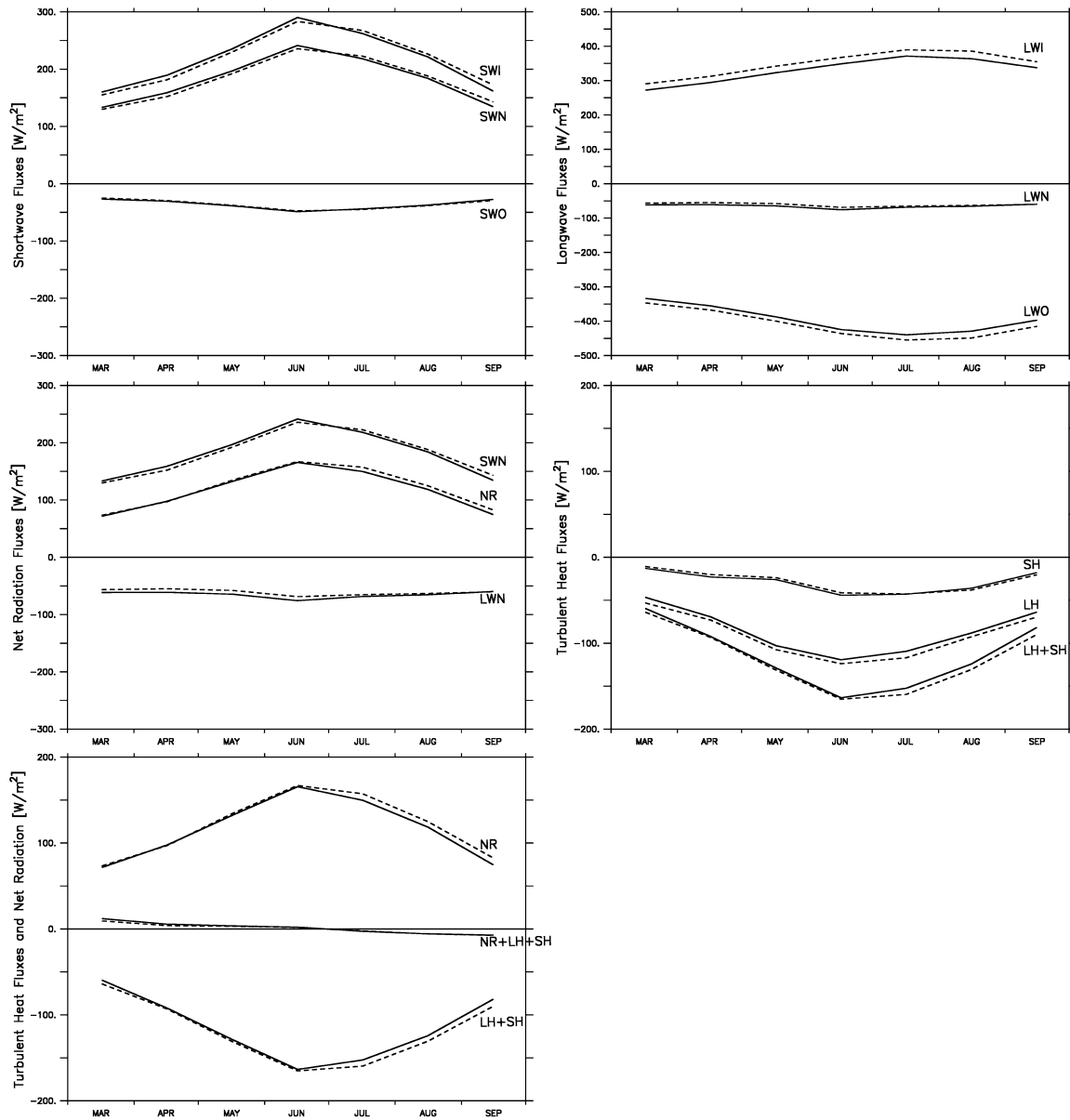


Fig. 12 Temporal evolution of the various components of the surface energy budget in the simulations CTL (*solid lines*) and WARM (*dashed lines*) over the Midwest (W/m^2). The values are spatial averages over the box outlined in Fig. 3. *SWI* denotes

incident shortwave (SW) radiation, *SWO* outgoing SW, *SWN* net SW, *LWI* incident longwave (LW) radiation, *LWO* outgoing LW, *LWN* net LW, *LH* latent heat flux, *SH* sensible heat flux, and *NR* net radiation. Downwards directed fluxes are counted as positive

greenhouse effect), while the change in the atmospheric CO_2 concentration has an almost negligible impact.

6 Summary and conclusions

The present study uses a regional climate model with a surrogate climate change scenario to investigate the mechanisms potentially leading to enhanced summer dryness in the Midwestern United States under warmer climatic conditions. The control integrations of four spring and summer seasons generally agree with observations in terms of their water cycle and precipitation distribution.

The WARM experiments are generally characterized by a wetter spring with enhanced convective activity (from March to June/July), followed by a period with somewhat drier climatic conditions (July–September). These changes are mostly induced by the modifications in temperature and humidity advection, rather than by local changes in atmospheric CO_2 concentrations. This is apparent from the comparison between the WARM and NOCO_2 experiments.

Although the summertime depletion of soil moisture in the WARM experiments is somewhat higher than in the CTL integrations, it is generally compensated by the higher infiltration in spring, when convective precipitation is enhanced. On average, the WARM integrations

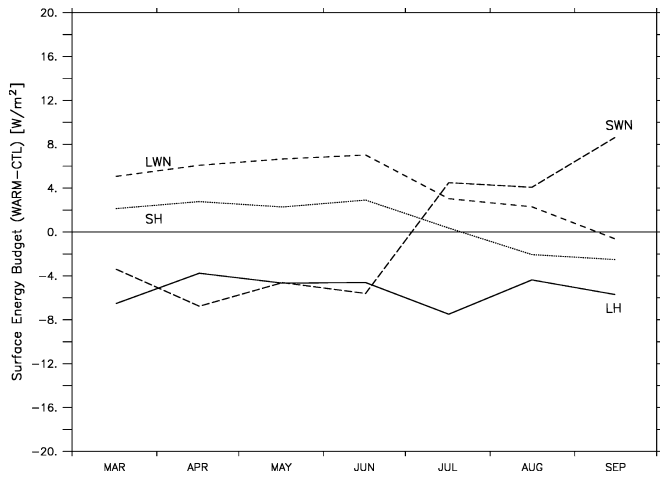


Fig. 13 Differences of various components of the surface energy budget between the CTL and WARM integrations over the Midwest in W/m^2 (WARM-CTL). The values are spatial averages over the box outlined in Fig. 3. *SWN* denotes net shortwave radiation, *LWN* net longwave radiation, *LH* the latent heat flux, and *SH* the sensible heat flux. Downwards directed fluxes are counted as positive

start showing weak signs of soil drying by late August only. There are, however, some noticeable year-to-year variations. In 1993, the flood year, the applied scenario leads to a net wetting of the soil. The highest drying is observed in 1990, a “normal” year, due to a decrease in large-scale precipitation in May.

Whether positive or negative, these soil moisture changes are nonetheless of very small magnitude (of the order of 1 to 2% of saturation at most); in this light, even the drying occurring in the 1990 experiment would thus represent a rather mild scenario. Overall, our results suggest that the risks of enhanced drying might possibly be smaller than suggested by earlier studies (e.g. WM95, Kattenberg et al. 1996).

The relatively mild changes observed in our simulations can mainly be explained by two factors. First, the soil is not fully saturated in spring and can thus absorb extra precipitation occurring during this season. In contrast, in the simulations of WM95, there are no compensating effects for the increases in evapotranspiration, as most of the enhanced spring precipitation is lost to runoff. Second and perhaps more importantly, increases in evapotranspiration are relatively moderate, thus restricting soil moisture depletion occurring in

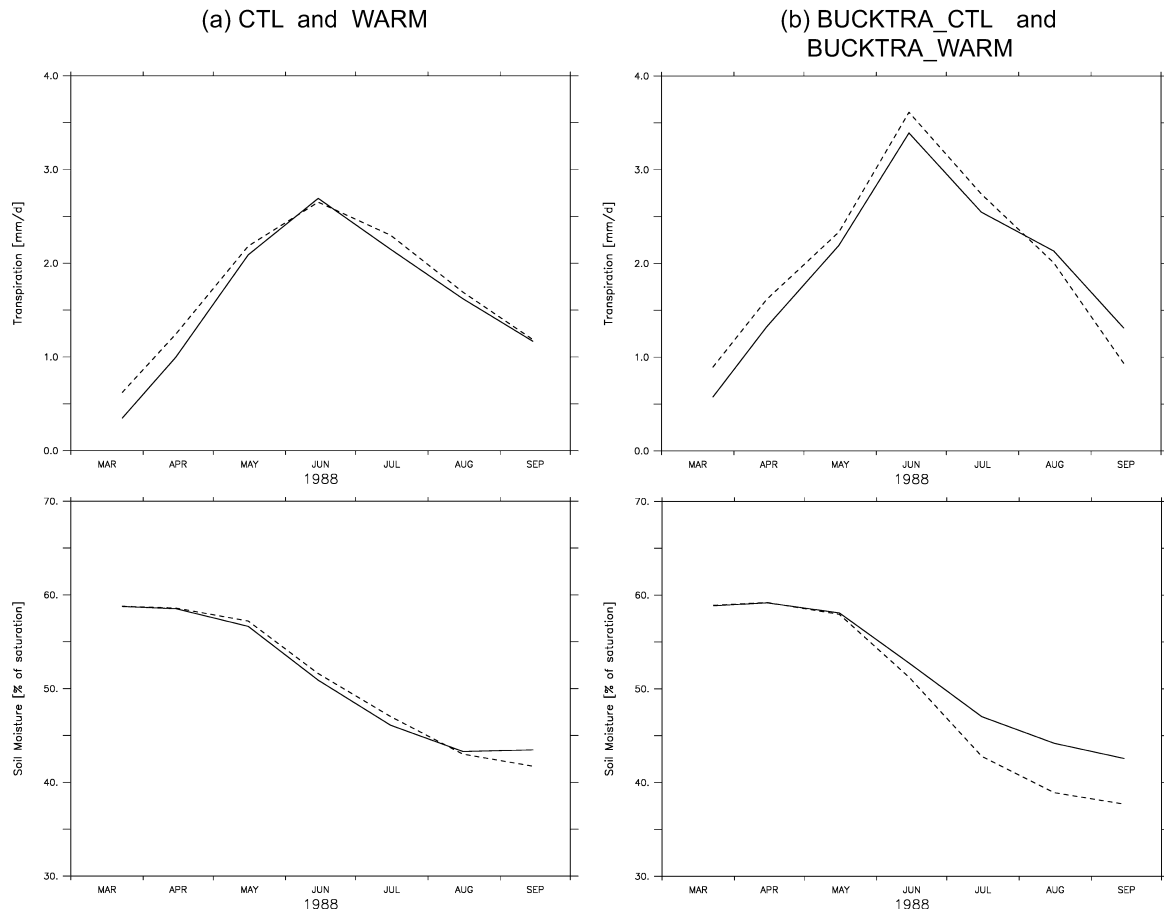


Fig. 14a, b Temporal evolution of transpiration (mm/d) (top) and soil moisture content in the root zone (% of saturation) (bottom) in 1988: **a** Simulations CTL (solid) and WARM (dashed); **b**

Simulations BUCKTRA_CTL (solid) and BUCKTRA_WARM (dashed). The values are spatial averages over the Midwest subdomain (outlined in Fig. 3)

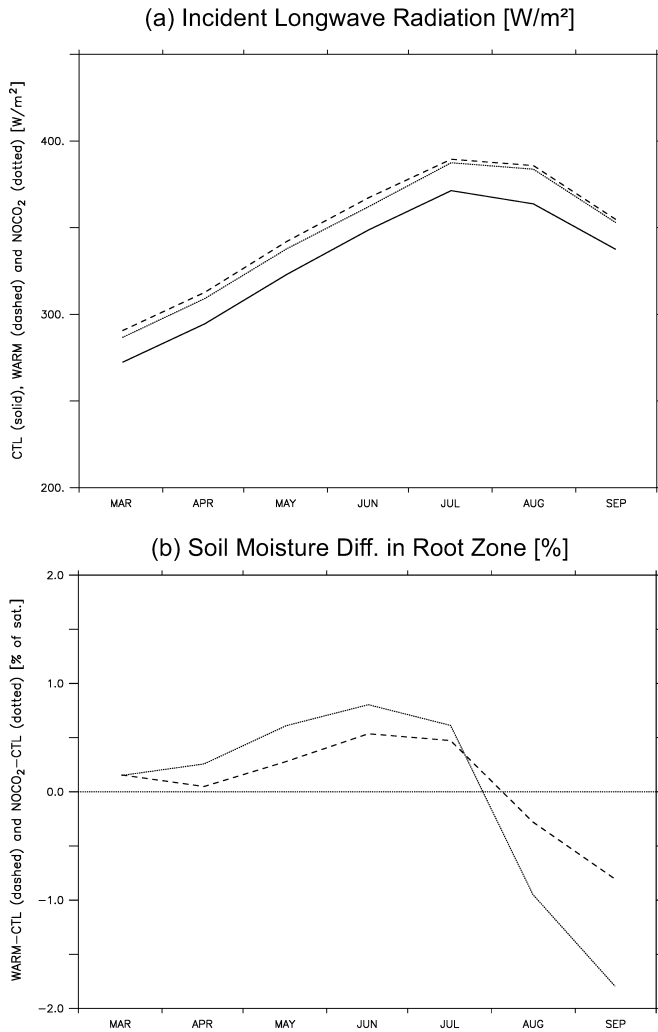


Fig. 15 **a** Temporal evolution of the incident longwave radiation in the simulations CTL (solid line), WARM (dashed line), and NOCO₂ (dotted line) in W/m² (average over all years). **b** Temporal evolution of the soil moisture differences in the root zone for WARM-CTL (dashed line) and NOCO₂-CTL (dotted line) in % of saturation (average over all years). The values are spatial averages over the box outlined in Fig. 3

summer. This behaviour appears to be tied to the use of a land-surface scheme of intermediate complexity (BATS). The simpler ‘bucket model’ as used in earlier studies is known to generally overestimate latent heat flux in various regimes (see Introduction), a fact which might exaggerate the simulated summer drying in some climate change simulations. This problem was also recognized by WM95, who stated: “In assessing the present results, one should recognize that the GCM used here employs a simple bucket model parametrization of land-surface processes. Because of this simplified formulation, it is possible that the midlatitude summer dryness discussed in this study may not be realized in the actual climate system”. Since our model uses a more sophisticated representation of the land-surface processes, it is possible that the mild changes observed in our simulations might be closer to reality. The results of the

BUCKTRA experiments, in which the BATS parametrization of transpiration was replaced with a bucket-type formulation, seem to confirm this hypothesis. They display a considerable drying in 1988, the drought year, which suggests that vegetation control on transpiration (through the stomatal and root resistances) might play an important part in counteracting an enhancement of summer drying when soil water gets scarce.

However, also our simulations entail various simplifications, which might question some of the results. First, our methodology does not allow for global changes in the synoptic-scale circulation patterns. Possible shifts in the storm tracks could be important features of climate change and are at present still difficult to predict (e.g. Kattenberg et al. 1996; Cubasch et al. 2001). Second, the simulations are only performed for the spring and summer seasons; it is possible that changes in fall precipitation or in the onset of snowmelt could significantly impact the hydrological cycle in warmer climatic conditions. Third, slight moisture deficits such as those displayed by the WARM experiments towards the end of the summer might add up and lead to a stronger drying in multi-year simulations. Last, some factors which were not accounted for in the present simulations (e.g. changes in aerosol concentrations, adaptive response of vegetation to climate change) could also be of relevance for this issue. Potential vegetation feedbacks which were not investigated here, such as changes in stomatal resistance (e.g. Henderson-Sellers et al. 1995), rooting depth (Milly 1997) and plant physiology (e.g. Sellers et al. 1996), or shifts in vegetation distribution patterns (e.g. Betts et al. 1997; Levis et al. 2000), might be of key importance in modulating the response of the climate system to changes in greenhouse gases and local climate.

Despite the aforementioned limitations, our study underlines the importance of land-surface processes in climate integrations, and the potential role of enhanced spring precipitation in substantially reducing a possible enhancement of summer dryness in mid-latitudes.

Acknowledgements We would like to acknowledge and thank Eric Small for his very valuable assistance at the beginning of this study. Many thanks are due to Christoph Frei, Oliver Fuhrer, Reto Stöckli, Pier Luigi Vidale, Pedro Viterbo and Martin Wild for their very helpful comments and suggestions. We would also like to express our sincere thanks to Richard Wetherald for kindly providing us with the data of the WM95 study as well as for his pertinent and constructive comments, which substantially contributed to improving the manuscript. Useful comments from an anonymous reviewer are also gratefully acknowledged. Special thanks are due to Eric Müller (Computing Services ETH) for technical support. In addition, we thank Filippo Giorgi for providing RegCM, Erik Kluzek (NCAR) for providing the framework necessary to implement the NCEP Reanalysis boundary conditions, NOAA-CIRES Climate Diagnostics Center for providing the NCEP Reanalysis data, and Daniel Lüthi for aid with the implementation of the rotated Mercator projection in the model and the generation of NetCDF output. Financial support for this study was provided by the MIT/ETH/UT Alliance for Global Sustainability, and by the Swiss National Science Foundation through the NCCR Climate Programme.

References

- Anthes R, Hsie E, Kuo Y (1987) Description of the Penn State/NCAR Mesoscale Model Version 4 (MM4). Technical report TN-282+STR, NCAR, Boulder, Colorado, USA, pp 66
- Arakawa A, Schubert WH (1974) Interaction of a cumulus cloud ensemble with the large-scale environment, Part I. *J Atmos Sci* 31: 674–701
- Betts AK, Ball JH, Beljaars ACM, Miller MJ, Viterbo PA (1996) The land-surface atmosphere interaction: a review based on observational and global modeling perspectives. *J Geophys Res* D101: 7209–7225
- Betts RA, Cox PM, Lee SE, Woodward FI (1997) Contrasting physiological and structural vegetation feedbacks in climate change simulations. *Nature* 387: 796–799
- Budyko MI (1974) *Climate and life*. Academic Press, New York, pp 510
- Cubasch U, Meehl GA, Boer GJ, Stouffer RJ, Dix M, Noda A, Senior CA, Raper S, Yap KS (2001) Projections of future climate change. In: Houghton JT and others (eds) *Climate change 2001: the scientific basis. Contribution of working group I to the third assessment report of the Intergovernmental Panel on Climate Change*. Cambridge University Press, Cambridge, UK, pp 525–582
- Davies HC, Turner R (1977) Updating prediction models by dynamical relaxation: an examination of the technique. *Q J R Meteorol Soc* 103: 225–245
- Déqué M, Marquet P, Jones RG (1998) Simulation of climate change over Europe using a global variable resolution general circulation model. *Clim Dyn* 14: 173–189
- Dickinson RE, Henderson-Sellers A (1988) Modelling tropical deforestation: A study of GCM land-surface parametrizations. *Q J R Meteorol Soc* 114: 439–462
- Dickinson RE, Henderson-Sellers A, Kennedy PJ (1993) Biosphere-atmosphere transfer scheme (BATS) version 1e as coupled to the NCAR community climate model. NCAR technical note, pp 72
- Dorman JL, Sellers PJ (1989) A global climatology of albedo, roughness length and stomatal resistance for atmospheric general circulation models as represented by the simple biosphere model (SiB). *J Appl Meteorol* 28: 833–855
- Easterling DR, Meehl GA, Parmesan C, Changnon SA, Karl TR, Mearns LO (2000) Climate extremes: observations, modeling, and impacts. *Science* 289: 2068–2074
- Findell KL, Eltahir EAB (1997) An analysis of the soil moisture-rainfall feedback, based on direct observations from Illinois. *Water Resour Res* 33: 725–735
- Frei C, Schär C, Lüthi D, Davies HC (1998) Heavy precipitation processes in a warmer climate. *Geophys Res Lett* 25(9): 1431–1434
- Fritsch JM, Chappell CF (1980) Numerical prediction of convectively driven mesoscale pressure systems. Part I: convective parametrization. *J Atmos Sci* 37: 1722–1733
- Garratt JR, O'Brien DM, Dix MR, Murphy JM, Stephens GL, Wild M (1999) Surface radiation fluxes in transient climate simulations. *Global Planet Change* 20: 33–55
- Gates WL, Henderson-Sellers A, Boer GJ, Folland CK, Kitoh A, McAvaney BJ, Semazzi F, Smith N, Weaver AJ, Zeng QC (1996) Climate models – evaluation. In: Houghton JT and others (eds) *Climate change 1995, The science of climate change. Contribution of working group I to the second assessment report of the Intergovernmental Panel on Climate Change*. Cambridge University Press, Cambridge, UK, pp 285–357
- Giorgi F, Marinucci MR, Bates GT (1993a) Development of a second-generation regional climate model (RegCM2). Part I: boundary-layer and radiative transfer processes. *Mon Weather Rev* 121(10): 2794–2813
- Giorgi F, Marinucci MR, Bates GT, De Canio G (1993b) Development of a second-generation regional climate model (RegCM2). Part II: convective processes and assimilation of lateral boundary conditions. *Mon Weather Rev* 121(10): 2814–2832
- Giorgi F, Mearns LO (1999) Introduction to special section: regional climate modeling revisited. *J Geophys Res* 104(D6): 6335–6352
- Gregory JM, Mitchell JFB, Brady AJ (1997) Summer drought in Northern midlatitudes in a time-dependent CO₂ climate experiment. *J Clim* 10: 662–686
- Grell G (1993) Prognostic evaluation of assumptions used by cumulus parametrizations. *Mon Weather Rev* 121: 764–787
- Grell GA, Dudhia J, Stauffer DR (1994) A description of the fifth generation Penn State/NCAR Mesoscale Model (MM5). NCAR Technical Note, NCAR/TN-398+STR, pp 121
- Heck P, Lüthi D, Wernli H, Schär C (2001) Climate impacts of European-scale anthropogenic vegetation changes: a sensitivity study using a regional climate model. *J Geophys Res Atmos* 106(D8): 7817–7835
- Henderson-Sellers A, McGuffie K, Gross C (1995) Sensitivity of global climate model simulations to increased stomatal resistance and CO₂ increases. *J Clim* 8: 1738–1756
- Henderson-Sellers A, McGuffie K, Pitman AK (1996) The project for intercomparison of land-surface parametrization schemes (PILPS): 1992 to 1995. *Clim Dyn* 12: 849–859
- Hollinger SE, Isard SA (1994) A soil moisture climatology of Illinois. *J Clim* 4: 822–833
- Holtlag AAM, de Bruijn EIF, Pan HL (1990) A high resolution of air mass transformation model for short-range weather forecasting. *Mon Weather Rev* 118: 1561–1575
- Huang J, van den Dool HM, Georgakakos K (1996) Analysis of model-calculated soil moisture over the US (1931–93) and application in long-range temperature forecasts. *J Clim* 9: 1350–1362
- Jacquemin B, Noilhan J (1990) Sensitivity study and validation of a land surface parameterization using the HAPEX-MOBILHY data set. *Boundary-Layer Meteorol* 52: 93–134
- Jarvis P (1976) The interpretation of the variations in leaf water potential and stomatal conductance found in canopies in the field. *Philos Trans R S London B* 273: 593–610
- Karl TR, Williams Jr TN, Quinlan TN, Boden TA (1990) United States Historical Climate Network (HCN) serial temperature and precipitation data. Technical Report Environmental Science Division, Publication No. 3404, Oak Ridge National Laboratory, Oak Ridge, TN, USA, pp 389
- Kattenberg A, Giorgi F, Grassl H, Meehl GA, Mitchell JFB, Stouffer RJ, Tokioka T, Weaver AJ, Wigley TML (1996) Climate models – projections of future climate. In: Houghton JT and others (eds) *Climate change 1995, the science of climate change. Contribution of working group I to the second assessment report of the Intergovernmental Panel on Climate Change*. Cambridge University Press, Cambridge, UK, pp 285–357
- Kiehl JT, Hack JJ, Bonan GB, Boville BA, Williamson DL, Rasch PJ (1998) The National Center for Atmospheric Research Community Climate Model: CCM3. *J Clim* 11: 1131–1149
- Kunkel K, Changnon S, Angel J (1994) Climate aspects of the 1993 Upper Mississippi River Basin flood. *Bull Am Meteorol Soc* 75: 811–822
- Levis S, Foley J, Pollard D (2000) Large-scale vegetation feedbacks on a doubled CO₂ climate. *J Clim* 13: 1313–1325
- Machenhauer B, Windelband M, Botzet M, Christensen JH, Déqué M, Jones RG, Ruti PM, Visconti G (1998) Validation and analysis of regional present-day climate and climate change simulations over Europe. MPI Report 275, Max Planck Institute, Hamburg, Germany, pp 87
- Manabe S (1969) Climate and ocean circulation. Part I: the atmospheric circulation and the hydrology of the earth's surface. *Mon Weather Rev* 97: 739–774
- Manabe S, Wetherald RT, Stouffer RJ (1981) Summer dryness due to an increase of atmospheric CO₂ concentrations. *Clim Change* 3: 347–386
- Milly PCD (1997) Sensitivity of greenhouse summer dryness to changes in plant rooting characteristics. *Geophys Res Lett* 24(3): 269–271
- Mo KC, Noguez Paegle J, Higgins RW (1997) Atmospheric processes associated with summer floods and droughts in the central United States. *J Clim* 10: 3028–3046

- Pal JS (2001) Modeling of the soil moisture-rainfall feedback mechanism. PhD Thesis, MIT, Cambridge, USA
- Pal JS, Eltahir EAB (2001) Pathways relating soil moisture conditions to future summer rainfall within a model of the land-atmosphere system *J Clim* 14: 1227–1242
- Pal JS, Small EE, Eltahir EAB (2000) Simulation of regional scale water and energy budgets: Importance of subgrid cloud and precipitation processes within RegCM. *J Geophys Res* 105(D24): 29,579–29,594
- Ramanathan V (1981) The role of ocean-atmosphere interactions in the CO₂ climate problem. *J Atmos Sci* 38: 918–930
- Raval A, Ramanathan V (1989) Observational determination of the greenhouse effect. *Nature* 342: 758–761
- Rind D, Chiou EW, Chu W, Larsen J, Oltmans S, Lerner J, McCormick MP, McMaster L (1991) Positive water vapour feedback in climate models confirmed by satellite data. *Nature* 349: 500–503
- Rind D, Goldberg R, Hansen J, Rosenzweig C, Ruedy R (1990) Potential evapotranspiration and the likelihood of future drought. *J Geophys Res* 95(D7): 9983–10,004
- Ropelewski CF (1988) The global climate for June–August 1988: a swing to the positive phase of the Southern Oscillation, drought in the United States and abundant rain in monsoon areas. *J Clim* 1: 1153–1174
- Rowntree PR (1991) Atmospheric parametrization schemes for evaporation over land: basic concepts and climate modeling aspects. In: Schmugge TS, André JC (eds) *Land surface evaporation*. Springer, New York Heidelberg Berlin, pp 5–29
- Schär C, Frei C, Lüthi D, Davies HC (1996) Surrogate climate-change scenarios for regional climate models. *Geophys Res Lett* 23(6): 669–672
- Schär C, Lüthi D, Beyerle U, Heise E (1999) The soil-precipitation feedback: a process study with a regional climate model. *J Clim* 12: 722–741
- Sellers PJ, Bounoua L, Collatz GJ, Randall DA, Dazlich DA, Los SO, Berry JB, Fung I, Tucker CJ, Field CB, Jensen TJ (1996) Comparison of radiative and physiological effects of doubled atmospheric CO₂ on climate. *Science* 271: 1402–1406
- Viterbo P (1996) The representation of surface processes in general circulation models. PhD Thesis, ECMWF, Reading, UK
- Wetherald RT, Manabe S (1995) The mechanisms of summer dryness induced by greenhouse warming. *J Clim* 8: 3096–3108
- Wetherald RT, Manabe S (1999) Detectability of summer dryness caused by greenhouse warming. *Clim Change* 43: 495–511
- Wild M, Ohmura A, Gilgen H, Roeckner E (1995) Regional climate simulation with a high-resolution GCM: surface-radiative fluxes. *Clim Dyn* 11: 469–486
- Wild M, Dümenil L, Schulz JP (1996) Regional climate simulation with a high-resolution GCM: surface-hydrology. *Clim Dyn* 12: 755–774
- Yeh PJF, Irizarry M, Eltahir EAB (1998) Hydroclimatology of Illinois: a comparison of monthly evaporation estimates based on atmospheric water balance and soil water balance. *J Geophys Res* 103(D16): 19,823–19,837